

# Synthesis, Characterization, and Magnetic Studies of Nonagglomerated Zerovalent Iron Particles. Unexpected Size Dependence of the Structure

Dominique de Caro, Teyeb Ould Ely, Alain Mari, and Bruno Chaudret\*

*Laboratoire de Chimie de Coordination du CNRS, UPR 8241 liée par convention à l'Université Paul Sabatier et à l'Institut National Polytechnique de Toulouse, 205, route de Narbonne, 31077 Toulouse Cedex, France*

Etienne Snoeck

*CEMES-LOE-CNRS, 29, rue Jeanne Marvig, BP 4347, 31055 Toulouse Cedex, France*

Marc Respaud, Jean-Marc Broto, and André Fert\*

*Laboratoire de Physique des Solides de l'Institut National des Sciences Appliquées, Complexe Scientifique de Rangueil, 31077 Toulouse Cedex, France*

Received December 15, 1995. Revised Manuscript Received March 8, 1996<sup>®</sup>

Sonolysis of a solution of  $\text{Fe}(\text{CO})_5$  in anisol in the presence of poly(dimethylphenylene oxide) (PPO) leads to the formation of small nonagglomerated iron particles. HRTEM analysis shows that the size of the particles is centered around 30 Å with a medium dispersity. HRTEM analysis of the particles demonstrate that the smaller particles ( $\leq 25$  Å) adopt the  $\alpha$ -Fe (bcc) structure, whereas the larger ones ( $\geq 25$  Å) adopt the  $\gamma$ -Fe (fcc) structure. Magnetic measurements confirm the presence of small superparamagnetic particles ( $\alpha$ -Fe) and of mostly antiferromagnetic or paramagnetic particles ( $\gamma$ -Fe).

The synthesis of nonagglomerated magnetic nanoparticles of controlled size, structure, and surface is an important challenge in materials science.<sup>1–3</sup> Thus, the facile preparation of such materials would allow the study of the fundamental properties of these nanoparticles, for example, the size dependence of their magnetic behavior (magnetic moment enhancement at the surface) and the possibility of long-range magnetic order.<sup>4</sup> Furthermore, numerous applications of these materials can be expected, for example, magnetic recording or permanent magnets, as long as they can be handled easily and their physical properties are stable with time.<sup>3</sup>

As far as the synthesis of small iron particles is concerned, several procedures have been described which lead to partially or totally oxidized materials.<sup>5</sup> Some methods have however been reported recently which described the synthesis of such zerovalent particles. This includes metal vapor deposition<sup>2</sup> and reduction of  $\text{FeCl}_3$  in inverse micelles, a method leading to

monodisperse, zerovalent iron particles with sizes varying according to the micelles from 14 to 125 Å.<sup>3</sup> An alternative method employing an organometallic precursor, namely, sonication of  $\text{Fe}(\text{CO})_5$ , has been discovered by Suslick and has led to agglomerated, amorphous iron particles.<sup>6</sup> Furthermore,  $\text{CO}_2$  laser-induced pyrolysis of  $\text{Fe}(\text{CO})_5$  has led to pure  $\gamma$ -Fe particles deposited into organic solvents with sizes ranging from 30 to 85 nm.<sup>7</sup>

We have recently shown that stable nonagglomerated colloids of zerovalent platinum group metal or coinage metal could be prepared by low-temperature decomposition of organometallic precursors in the presence of a reactive gas (CO or  $\text{H}_2$ ).<sup>8</sup> The advantage of the method lies in the absence of possible contaminants linked to the use of chemical reductants (alkali metals, halogens, boron, etc.). The synthesis of magnetic particles is however more challenging because of the easy oxidation and agglomeration of these particles.

We describe hereafter preliminary results concerning the synthesis and magnetic properties of zerovalent iron

<sup>®</sup> Abstract published in *Advance ACS Abstracts*, July 15, 1996.

(1) Gibson, C. P.; Putzer, K. J. *Science* **1995**, 267, 1338.

(2) (a) Easom, K. A.; Klabunde, K. J.; Sorensen, C. M.; Hadjipanayis, G. C. *Polyhedron* **1994**, 13, 1197 and references therein. (b) Kernizan, C. F.; Klabunde, K. J.; Sorensen, C. M.; Hadjipanayis, G. C. *Chem. Mater.* **1990**, 2, 70.

(3) (a) Venturini, E. L.; Wilcoxon, J. P.; Newcomer, P. P. *Mater. Res. Soc. Symp. Proc.* **1994**, 351, 311. (b) Wilcoxon, J. P.; Williamson, R. L.; Baughman, R. J. *J. Chem. Phys.* **1993**, 98, 9933.

(4) (a) Bucher, J. P.; Douglas, D. C.; Bloomfield, L. A. *Phys. Rev. Lett.* **1991**, 66, 3052. (b) Alden, M.; Mirbt, S.; Skriver, H. L.; Rosengaard, N. M.; Johansson, B. *Phys. Rev. B* **1992**, 46, 6303.

(5) (a) Bridger, K.; Watts, J.; Tadros, M.; Gang Xiao; Liou, S. H.; Chien, C. L. *J. Appl. Phys.* **1987**, 61, 3323. (b) Jung, C.; Rybicki, E.; Raghavan, S.; Mathur, M. C. A. *Colloids Surf. A* **1993**, 80, 77.

(6) (a) Suslick, K. S.; Choe, S. B.; Cichowlas, A.; Grinstaff, M. *Nature* **1991**, 353, 414. (b) Grinstaff, M. W.; Salamon, M. B.; Suslick, K. S. *Phys. Rev. B* **1993**, 48, 269.

(7) Zhao, X. Q.; Zheng, F.; Liang, Y.; Hu, Z. Q.; Xu, Y. B. *Mater. Lett.* **1994**, 21, 285.

(8) (a) Duteil, A.; Queau, R.; Chaudret, B.; Mazel, R.; Roucau, C.; Bradley, J. S. *Chem. Mater.* **1993**, 5, 341. (b) de Caro, D.; Wally, H.; Amiens, C.; Chaudret, B. *J. Chem. Soc., Chem. Commun.* **1994**, 1891. (c) Amiens, C.; de Caro, D.; Chaudret, B.; Bradley, J. S.; Mazel, R.; Roucau, C. *J. Am. Chem. Soc.* **1993**, 115, 11638. (d) de Caro, D.; Agelou, V.; Duteil, A.; Chaudret, B.; Mazel, R.; Roucau, C.; Bradley, J. S. *New. J. Chem.*, in press.

nanoparticles stabilized by polymers and the observation of a surprising size dependence of the structure of the particles.

The organometallic precursors used in this study were the bis(cyclooctatetraene) complex  $\text{Fe}(\text{C}_8\text{H}_8)_2$  (**1**)<sup>9</sup> and  $\text{Fe}(\text{CO})_5$  (**2**) previously used by Suslick.<sup>6</sup> Unlike the corresponding ruthenium complex  $\text{Ru}(\eta^4\text{-C}_8\text{H}_{10})(\eta^6\text{-C}_8\text{H}_{12})$ , **1** does not readily decompose under 3 bar of  $\text{H}_2$  in the presence of poly(vinylpyrrolidone) (PVP). The reaction was carried out in different conditions (90, 75, 20 °C) for several days but always severely agglomerated materials were obtained except for very low metal content (*ca.* 2 wt % Fe in PVP) in which case some isolated particles with sizes ranging from 20 to 50 Å were visible by TEM. This negative result led us to attempt the decomposition of the commercially available complex  $\text{Fe}(\text{CO})_5$  (**2**) by sonication in the presence of PVP or poly(dimethylphenylene oxide) (PPO), a polymer recently shown to stabilize copper or gold particles.<sup>8d</sup> The sonication was carried out using a Vibra-Cell 20 kHz apparatus equipped with a titanium probe and operated at *ca.* 20% of the total power of the apparatus (60 W cm<sup>-2</sup>). Sonication in THF in the presence of PVP did not lead to decomposition of  $\text{Fe}(\text{CO})_5$ . However, when the reaction was carried out in anisole in the presence of PPO (initial conditions: [Fe] = 0.3 mol L<sup>-1</sup>; Fe/PPO = 170 wt %), the color of the solution changed rapidly from pale yellow to black in agreement with the decomposition of **2**.<sup>10</sup> An infrared spectrum of the crude residue obtained after solvent evaporation indicated the presence of several carbonyl iron species, most probably clusters displaying  $\nu_{\text{CO}}$  absorptions between 1800 and 2100 cm<sup>-1</sup>. Washing this residue under argon several times with THF resulted in the disappearance of these infrared bands and formation of a black material, soluble in anisole, and containing *ca.* 10 wt % iron as determined by microanalysis.

The distribution and the fine structure of the small particles were studied by high-resolution transmission electron microscopy (HREM) on a Philips CM30/ST microscope working at 300 kV with a point resolution of 1.9 Å. To study the particle size distribution over a large number of objects, image analyses were performed on digitized micrographs using the Optimas program.

Transmission electron microscopy (TEM) experiments evidence the presence of nonagglomerated small particles in the sample prepared in the presence of PPO. The histogram in Figure 1 shows a grain diameter distribution between 10 and 120 Å and centered around 30 Å. Assuming spherical particles, the log-normal size distribution gives an adequate description with a median radius in the range  $19 \pm 1$  Å and a standard deviation of  $\sigma = 5.5 \pm 0.5$ . However, TEM observations of the largest particles (diameter > 80 Å) reveal that

(9) Carbonaro, A.; Greco, A.; Dall'asta, G. *J. Organomet. Chem.* **1969**, *20*, 177.

(10) The sonolysis was carried out according to the following experimental procedure. Anisole was dried beforehand by passing through activated alumina and degassed after freezing in liquid  $\text{N}_2$ . The sonochemical reaction chamber was charged under argon with 1 mL  $\text{Fe}(\text{CO})_5$  (7.6 mmol, 425 mg of Fe) and with a solution of 250 mg PPO in 25 mL anisole. The yellow transparent solution thus obtained was then maintained under an argon pressure and submitted to ultrasounds. The color of the solution changed very rapidly from yellow to black. After 1 h, the solution was transferred under argon into 30 mL of pentane. A black precipitate was then obtained, washed with THF ( $2 \times 15$  mL) and dried under vacuum. The precipitate can be easily redissolved in anisole.

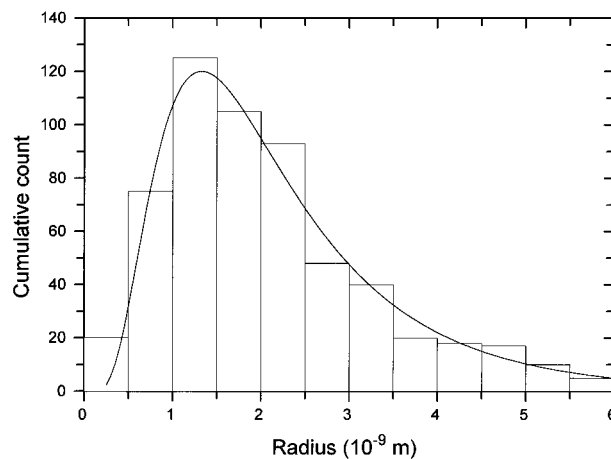


**Figure 1.** Experimental size distribution of Fe/PPO particles (full-line: log-normal size distribution).

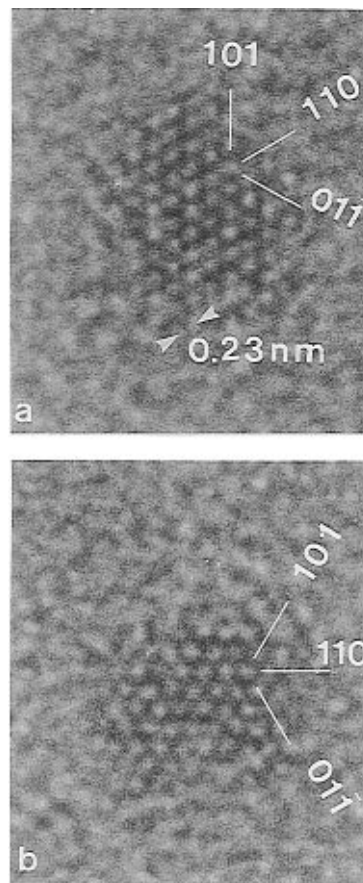


**Figure 2.** HREM micrographs of (a) 20 and (b) 25 Å diameter  $\alpha$ -Fe (bcc) particles.

most of these objects are polycrystalline and result from the agglomeration of several grains.

To clear up the structure of single small particles HREM experiments were carried out and Fourier transforms were computed on the HREM micrographs. Figure 2 shows HREM micrographs of isolated grains having a diameter of about 20 and 25 Å, respectively. The Fourier transform of these particles evidences three equivalent lattice spacings in three directions making an angle of 60° between them. The measurement of their interatomic spacing along one direction on the HREM images in Figure 2 gives 2.3 Å. The 3-fold symmetry observed on the images in Figure 2 and the lattice parameter of the particles suggest a bcc structure

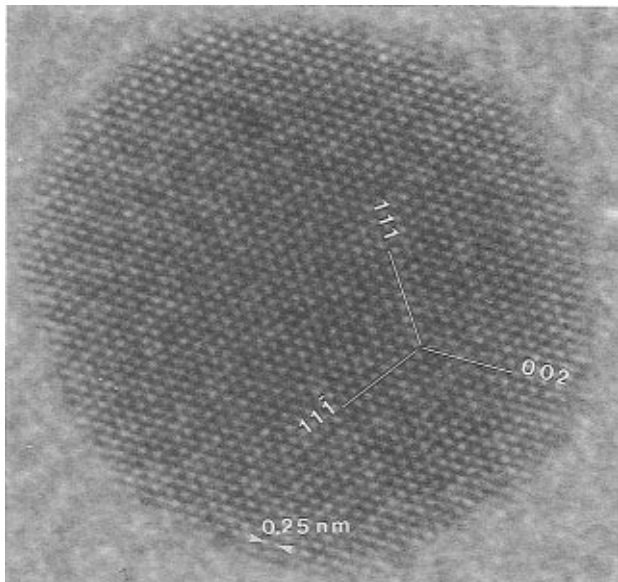


**Figure 3.** HREM micrograph of a 106 Å diameter  $\gamma$ -Fe (fcc) particle.

projected along the [111] direction which reveals the {110} planes. These small particles are then  $\alpha$ -Fe single crystals. However, larger single particles were also observed. One of them with a diameter of 105 Å is reported in Figure 3. The Fourier transform of this particle evidences two equivalent lattice spacings in two directions making an angle of about  $72^\circ$  and another one at  $56^\circ$  from the previous directions. This symmetry and the lattice distance measurements performed on the HREM micrographs indicate a  $\gamma$ -Fe (fcc) structure of the particle which is observed along a [110] zone axis showing up two {111} dense planes and a (002) one. Such fcc structure was regularly observed on particles of diameter larger than 30 Å.

HREM experiments show that the smallest Fe particles have a bcc structure while the larger ones exhibit a fcc one. Since the bulk  $\gamma$ -Fe (fcc) structure is stable only for temperature higher than 912 °C, the bcc structure being that stable at room temperature, the appearance of small Fe-fcc particles is surprising. The nucleation of this Fe-fcc phase could be due to the presence of very high local temperatures during the sonication process followed by a rapid quench avoiding any recrystallization processes. This is consistent with the appearance in the sonication process of high local temperatures and pressures established by Suslick.<sup>6</sup> The formation of Fe-bcc particles could occur in less severe conditions, suggesting that the medium is not homogeneous and displays a gradient of temperature. Another possibility is the presence inside our particles of interstitial carbon which would stabilize the  $\gamma$ -Fe phase.

**Magnetic Properties of the Particles.** The magnetic properties of iron ultrafine particles depend strongly on particle size, crystalline structure, and the presence of an oxidized shell.  $\alpha$ -Fe (bcc) particles have a ferromagnetic order despite the presence of an oxidized surface in some cases.<sup>11</sup> The weak magnetization compared to bulk  $\alpha$ -Fe has been attributed to either the

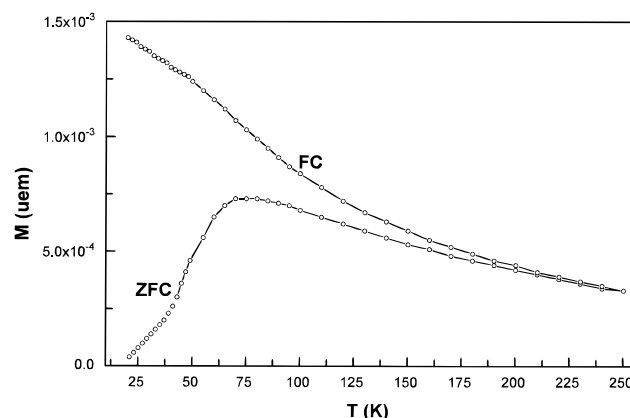


**Figure 4.** Zero-field-cooled and field-cooled magnetization versus temperature for Fe/PPO particles.

presence of a dead layer on the particle surface or the canting of magnetic moments in the oxide shell.<sup>12</sup> On the other hand, contradictory results have been published on magnetic properties of fcc-Fe particles. In general, fcc-Fe particles present an antiferromagnetic order with a Néel temperature between 65 and 70 K<sup>13</sup> which lowers as the particle size decreases,<sup>14</sup> but they can also adopt a ferromagnetic order<sup>15</sup> or a paramagnetic behavior.<sup>16</sup> Ultrafine particles of magnetic compounds are typically superparamagnetic. In single-domain particles with uniaxial anisotropy, only two states can exist with a minimum energy corresponding to the magnetization parallel to the easy axis.<sup>17,18</sup> Superparamagnetism is due to thermal fluctuations of the magnetic moment switching from one stable position to another. The relaxation time is given approximately by  $\tau = (1/f_0)\exp(E/k_B T)$ , where  $f_0$  is a frequency typically of  $10^9$  Hz.  $E$  is the height of the energy barrier given by  $E = KV(1 - H/H_0)^2$  with  $H_0 = 2K/M_S$  where  $K$  is the first-order anisotropy constant,  $V$  the volume, and  $M_S$  the saturation magnetization of the switching unit. The applied field  $H$  is taken as positive when applying in the direction that tends to cause switching.

The magnetization studies were carried out using a MPMS 5.5 Quantum Design (with a SQUID detector). The temperature could be varied from 2 to 400 K, and magnetic fields up to 5.5 T were applied. For the magnetic measurements, powders obtained after precipitation and washing of the colloid solutions were transferred in an argon glovebox into a small container to preserve from any uncontrolled oxidation which was then introduced into the magnetometer.

The first signature of the superparamagnetic behavior is shown in Figure 4 where the magnetization versus

(12) (a) Berkowitz, A. E.; Schuele, W. J.; Flanders, P. J. *J. Appl. Phys.* **1968**, *39*, 1261. (b) Morish, A. H.; Haneda, K.; Schurer, P. J. *J. Phys. Colloq.* **1976**, *37*, C6–301. (c) Coey, J. M. D. *Phys. Rev. Lett.* **1972**, *27*, 1140. (d) Pankhurst, Q. A.; Pollard, R. J. *Phys. Rev. Lett.* **1991**, *67*, 248.

(13) (a) Abrahams, S. C.; Guttman, L.; Kasper, J. S. *Phys. Rev.* **1962**, *127*, 2052. (b) Panduani, C.; Da Silva, E. G. *J. Magn. Magn. Mater.* **1994**, *134*, 161.

(14) Ezawa, T.; Macedo, W. A. A.; Glos, U.; Keune, W.; Schletz, K. P.; Kirschbaum, U. *Physica B* **1989**, *161*, 281.

(15) (a) Tejada, J.; Balcells, Ll.; Zhang, X. X. *J. Magn. Magn. Mater.* **1993**, *118*, 65. (b) Keune, W.; Ezawa, T.; Macedo, W. A. A.; Glos, U.; Schletz, K. P.; Kirschbaum, U. *Physica B* **1989**, *161*, 269. (c) Moruzzi, V. L.; Marcus, P. M.; Kubler, J. *Phys. Rev. B* **1989**, *39*, 6957.

(16) Haneda, K.; Zhou, Z. X.; Morrish, A. H.; Majima, T.; Miyahara, T. *Phys. Rev. B* **1992**, *46*, 13832.

(17) Néel, L. *Ann. Geophys.* **1949**, *5*, 99.

(18) Bean, C. P.; Livingston, J. D. *J. Appl. Phys.* **1959**, *30*, 1205.

(11) Gangopadhyay, S.; Hadjipanayis, G. C.; Dale, B.; Sorensen, C. M.; Klabunde, K. J.; Papaefthymiou, V.; Kostikas, A. *Phys. Rev. B* **1992**, *45*, 9778.

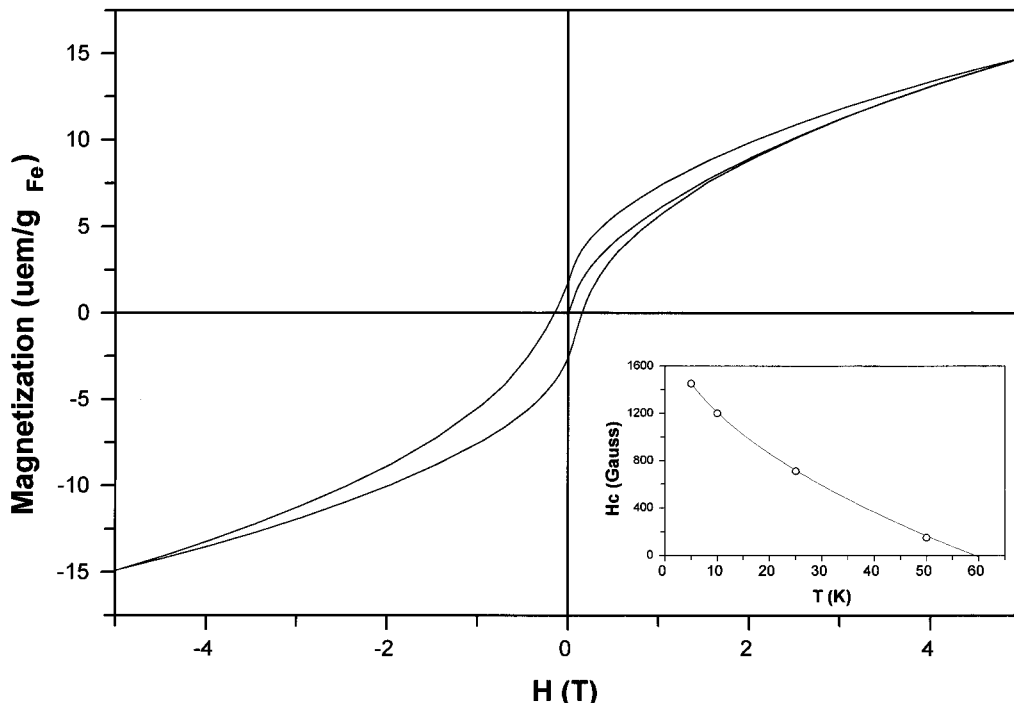


**Figure 5.** Hysteresis loop for Fe/PPO particles at 5 K (insert: coercive field plotted versus temperature).

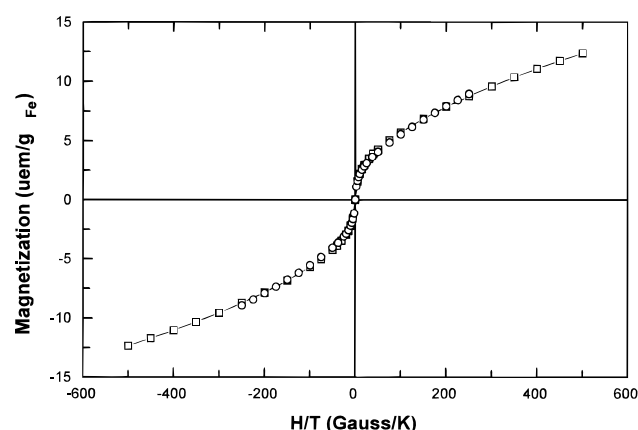
field is measured with an applied field of 10 G according to the zero field cooling (ZFC)/field cooling (FC) processes.<sup>19</sup> The ZFC magnetization shows a broad maximum at  $T_B = 75$  K and a large irreversibility in the field cooling (FC) process. The broad maximum reflects the existence of a large size distribution. As the temperature rises, the fraction of particles above their blocking temperature increases and the magnetization decreases according to a Curie law.

Figure 5 shows the hysteresis loop (magnetization versus applied magnetic field) at 5 K. The two major features are the absence of saturation in fields up to 5 T and the lower magnetization values compared to bulk bcc-iron. Below the blocking temperature, the sample shows hysteresis loops. The insert in Figure 5 shows the coercive field plotted versus temperature. This curve was fitted with the law  $H_C = H_C^0 (1 - aT^{1/2})$  which is used in the case of monodisperse noninteracting particles,<sup>18</sup> with  $H_C^0$  being the coercive field at absolute zero and  $a^2 = (k_B/KV)\ln(\tau_m/\tau_0)$ . If we compare this formula with those established by Néel, we may have  $a^2 = 1/T_B$ . In our case we find  $a^{-2} = 60 \pm 5$  K, which is in relative good agreement with  $T_B$  determined by ZFC.

Above the blocking temperature the hysteresis behavior disappears. Figure 6 shows the magnetization versus applied field divided by temperature for two different temperatures (100 K and 200 K). The data collapse on a single curve as expected for superparamagnetism for  $T > T_B$ .

The magnetic measurements allow us to eliminate the hypothesis of high-spin ferromagnetic ordered fcc particles. On the other hand, we cannot conclude on the type of magnetic behavior (antiferromagnetic or paramagnetic), both being compatible with the absence of saturation and weak magnetizations at 5 K.<sup>20</sup>

The superparamagnetism observed above 100 K and the magnetization in ZFC/FC process above 65/70 K



**Figure 6.** Magnetization versus applied magnetic field divided by temperature (100 K, squares; 200 K, circles).

take their origin in the presence of bcc particles, the atoms of fcc particles becoming or being paramagnetic. From  $T_B$  we can deduce the anisotropy constant  $K_{eff}$  for bcc particles, according to the law<sup>12</sup>  $K_{eff}V_m = 25k_B T_B$  where  $V_m$  is the mean volume and  $k_B = 1.38 \times 10^{-23}$  J/K. By taking  $V_m$  equal to a sphere of radius 1.5 nm, we find  $K_{eff} = 1.83 \times 10^6$  J/m<sup>3</sup>. A similar value was obtained by Xiao *et al.* for 2.5 nm iron particles,<sup>21</sup> which is very high compared to bulk value. Indeed, the magnetic anisotropy for small particles is mainly governed by shape and surface anisotropy and consequently much larger than expected for only crystalline anisotropy.

From the temperature where ZFC and FC curves collapse (around 210 K), we can deduce the maximum volume of bcc-iron particles according to the precedent

(20) (a) Dorman, J. L.; Ji Ren Cui, Sella, C. *J. Appl. Phys.* **1985**, 57, 4283. (b) Fiorani, D.; Romero, H.; Suber, L.; Testa, A. M.; Dorman, J. L.; Makani, J.; Spavieri, N. *J. Magn. Magn. Mater.* **1995**, 140–144, 411.

(21) Xiao, G.; Liou, S. H.; Levy, A.; Taylor, J. N.; Chien, C. L. *Phys. Rev. B* **1986**, 34, 7573.

law. It corresponds to a sphere of  $2.1 \pm 0.1$  nm radius. This result is consistent with HREM experiments.

### Conclusion

We report in this communication the facile synthesis of non-oxidized, nonagglomerated iron small particles. Although we did not find a suitable organometallic precursor for low-temperature decomposition, the sonolysis method originally developed by Suslick, but employed here in the presence of the polymer poly(dimethylphenylene oxide) (PPO), allowed the preparation of such particles. Most of iron present in the polymer

was found to adopt the nonthermodynamically stable  $\gamma$ -Fe (fcc) phase. However, the small particles were shown to adopt mainly the  $\alpha$ -Fe (bcc) structure. Furthermore, the magnetic properties of this material agrees with the presence of some small superparamagnetic  $\alpha$ -Fe (fcc) particles and a large amount of antiferromagnetic or paramagnetic  $\gamma$ -Fe (fcc) particles. The reasons for this size dependence of the structure are not clear. We are now looking for more suitable precursors allowing the selective synthesis of Fe(0) particles of either structure.

CM950599F